Density Functional Theory Investigation of Competitive Free-Radical Processes during the Thermal Cracking of Methylated Polyaromatics: Estimation of Kinetic Parameters

J-Philippe Leininger,[†,‡] Christian Minot,*[,‡] François Lorant,[†] and Françoise Behar[†]

Laboratoire de Chimie Théorique, Case 137, CNRS-UMR 7616, Université Pierre et Marie Curie, Paris VI 75252 Paris Cedex 05, France, and Division Géologie et Géochimie, Institut Français du Pétrole, 1-4 avenue de Bois-Préau, 92852 Rueil-Malmaison, France

Received: July 12, 2006; In Final Form: February 12, 2007

Density functional B3LYP and BH&HLYP calculations with the 6-31G** basis set have been performed to investigate elementary reactions playing an important role in the pyrolysis of 1-methylnaphthalene. The pathways describing the destiny of the main radicals, H, methyl, hydromethylnaphthyl and methylnaphthyl, have been studied. At low temperature, addition of H atoms on the aromatic ring is favored over hydrogen abstraction. Except at low temperature (below 400 K), the hydromethylnaphthyl radical undergoes preferentially a loss of hydrogen rather than a bimolecular hydrogen transfer with methylnaphthalene or addition reaction on methylnaphthalene forming a hydrogenated dimer. In the range 400−750 K, the formation of methane by hydrogen abstraction of methyl radical on methylnaphthalene is predominant compared to the formation of hydrodimethylnaphthalenes by addition reaction. Rate constants of reactions describing the formation of heavy products like methyldinaphthylmethanes or dimethylbinaphthalenes have been calculated and discussed. They are also compared to recombination reactions from the literature. Rate constants of these reactions have been computed using transition state theory and can be integrated in kinetic radical schemes of methylated polyaromatic compounds pyrolysis from geological to laboratory conditions.

1. Introduction

The thermal stability of aromatic compounds is a key parameter to understand the thermal evolution of oils in sedimentary basins[1] (at temperatures between 400 and 500 K and pressures ranging between 20 and 100 MPa), which is controlled by the kinetics of cracking reactions. Recent pyrolysis experiments[2−7] on methylated polyaromatics (between 600 and 700 K during few hours) representative of the main aromatic structures in oils have been performed to elucidate the complex thermal reactivity of this chemical class. Leininger et al.[7] proposed a set of the main processes involved in 1-methylnaphthalene thermal cracking, based on pyrolysis experiments of pure 1-methylnaphthalene. The rate constants of these elementary radical processes are needed in the 400−700 K temperature scale to obtain a radical kinetic scheme describing quantitalively the thermal decomposition of 1-methylnaphthalene from laboratory conditions (600−700 K/few hours) to the geological conditions (400−500 K/million years). Furthermore, among the radical elementary processes proposed, some of them were competitive and some uncertainties remained about the formation of heavy products. Hence, the calculation of the rate constants of the elementary processes would allow the discrimination between competitive reactions and preferential formations of heavy products. The purpose of this work is thus to calculate rate constants and kinetic parameters of selected radical processes and feed a predictive kinetic scheme of 1-methylnaphthalene thermal decomposition. However, no experimental thermokinetic data are available for such reactions on methylated polyaromatics and the use of group contribution methods for the estimation of the rate constants remains rough.

The use of quantum methods and transition state theory[8] can supply knowledge on rate constants of the elementary processes: it is possible to determine the rate constants of the reactions by derivation from calculations of vibration frequencies and localization of the transition state.[9−12] We propose to model the reactions displayed in Figure 1 and numbered from 1 to 9. They are displayed in three competitive pathways, A, B, and C, according to the nature of the radical initiating the reaction. The A pathway is the competition between the addition (1) and hydrogen abstraction (2) of H atoms on the reactant. The abstracted hydrogen can originate either from the aromatic ring or from the methyl group of methylnaphthalene.

The B pathway is linked to the destiny of the methylhydronaphthyl radical (HMNa). Three reactions can consume this radical: reaction 3, called radical hydrogen transfer (RHT), has been invoked to explain the reactivity of polycyclic aromatic hydrocarbons.[13−18] It corresponds to the migration of H atom between HMNa and 1-methylnaphthalene, notably to the ipso position of the methyl group (iHMNa). Thereafter the carbon−carbon bond dissociation between naphthalene and the methyl group of ipso methylhydronaphthyl radical is feasible[19] which leads to the formation of naphthalene. This reaction can be followed by hydrogen abstraction reactions (5) and (6) by the methyl radical on the reactant to form methane. Reaction 4, addition of the methylhydronaphthyl radical to the reactant to form a trihydrogenated-dimethylbinaphthyl radical (H_3D1), next contributes to release hydrogen in the system by successive dehydrogenation reactions. Another possibility of reaction of the pathway B is the reverse reaction of (1), the loss of hydrogen by unimolecular carbon-hydrogen dissociation.

The pathway C involves the methylnaphthyl radical (RMNa). This radical can undergo either hydrogen abstraction (7) or recombination forming respectively naphthylmethyl (MNRa)

* Corresponding author. E-mail: minot@lct.jussieu.fr.
† Institut Français du Pétrole.
‡ Université Pierre et Marie Curie.

10.1021/jp0643956 CCC: $37.00
Published on Web 03/30/2007

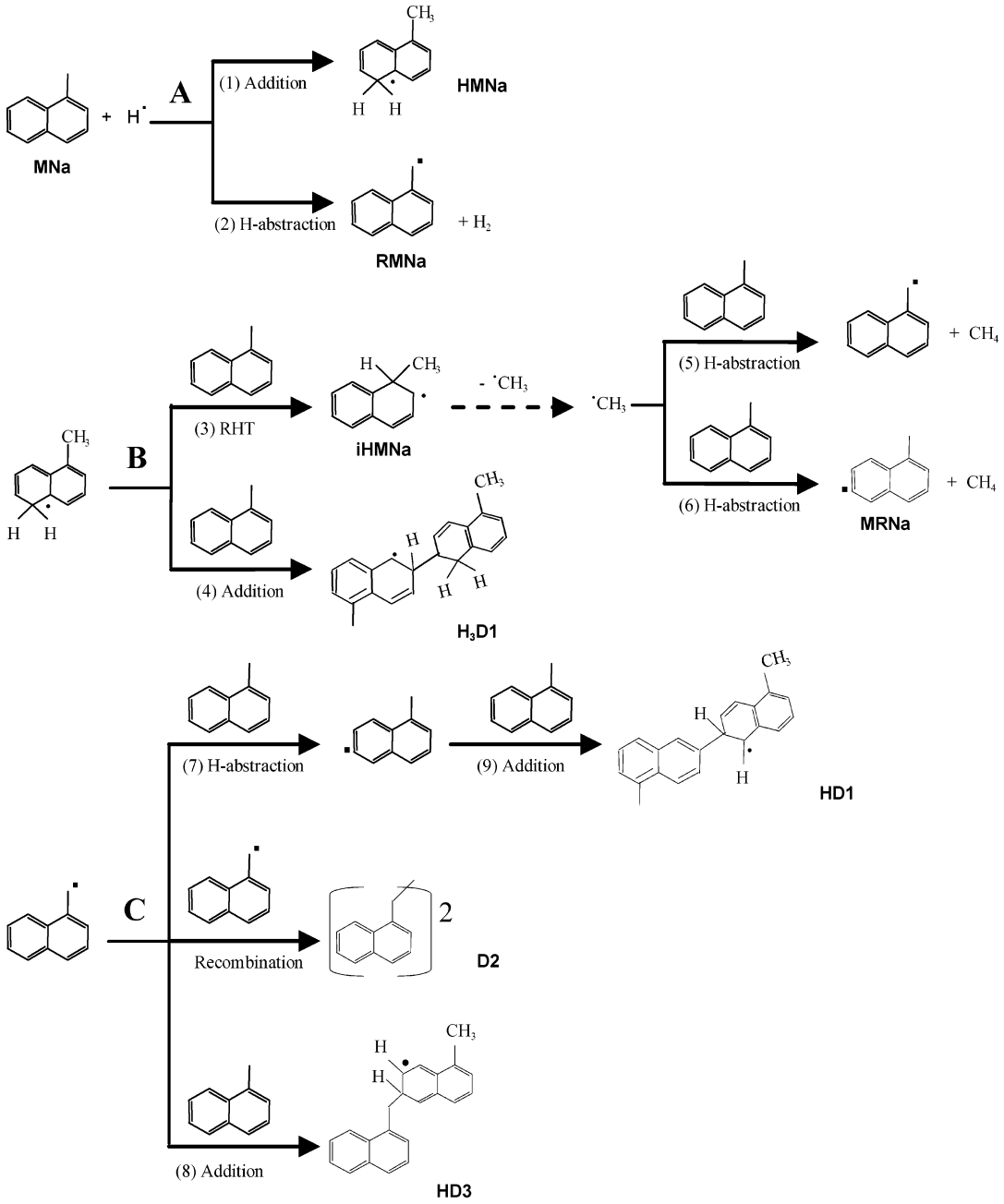

Figure 1. Competitive radical reactions thought to play an important role in 1-methylnaphthalene thermal cracking (reproduced from Leininger et al.[7]).

and 1,1′-dinaphthylethane (D2) radicals. RMNa radicals can also undergo an addition reaction on 1-MNa (8), forming hydromethyldinaphthylmethane, called HD3. MNRa radical formed by (7) can react on 1-methylnaphthalene by addition reaction (9) and form a hydrogenated dimethylbinaphthyl radical (HD1). Thereafter we will discuss the relevance of each reaction within the kinetic schemes addressed.

2. Computational Methods

All of the electronic structure calculations were carried out with the Jaguar v5.5 and v6.5 program[20] within the DFT[21] framework. Considering the high consuming time needed for calculations on such large systems (up to 43 atoms) the choice was made to calculate the optimized geometries and harmonic vibrational frequencies using the hybrid density functional uB3LYP[22,23] method with the 6-31G(d,p) basis set.[24] For addition/elimination reactions, we have used the B3LYP functional that led to accurate values for similar reactions on hydrocarbon systems.[25−33] For hydrogen abstraction reactions, BH&HLYP was used for single point energy calculations of reactant, products, and the transition state of hydrogen abstraction reactions from geometries calculated with B3LYP for hydrogen abstraction reactions. The BH&HLYP[34−36] functional has indeed been suggested to give better energy barriers[37−41] in spite of poorer bond energies and energies of reaction.[39,40] This approach provides a viable alternative to more computationally intensive methods for our large systems.

Reaction rate constants were estimated using the transition state theory[8] (TST) according to the following formula:

$$k^{\ddagger} = \kappa(T)\left(\frac{p_0}{R'T_0}\right)^{-m}(k_b T/h)\exp(-\Delta G_0^{\ddagger}/RT) \qquad \text{(i)}$$

where $\kappa(T)$ is the tunneling corrections term, T_0 and P_0 are the

TABLE 1: Spin Contamination of Reactants, Products, Transition States, and Imaginary Frequencies of TS Calculated at uB3LYP/6-31G; Barrier Heights Calculated at uB3LYP/6-31G** or uBH&HLYP/6-31G**; and Heats of Reactions Calculated at the uB3LYP/6-31G** Level of Theory**

reaction		structure	$\langle S^2 \rangle$	iw, cm^{-1}	heats of reaction + ZPE corrections (kcal/mol)	barrier Heights + ZPE and BSSE corrections (kcal/mol)
I	H addition	reactant	0.75			
		product	0.789			B3LYP
		TS_1	0.764	−696	−26.6	4.4
2	H-abstraction	reactant	0.75			
		product	0.795			BH&HLYP
		TS_2	0.766	−1169	−16.4	7.4
3	RHT	reactant	0.788			
		product	0.783			BH&HLYP
		TS_3	0.804	−1896	−1.6	26.5
4	C−C addition	reactant	0.754			
		product	0.795			B3LYP
		TS_4	0.769	−516	10.3	23.1
5	H-abstraction	reactant	0.783			
		product	0.788			BH&HLYP
		TS_5	0.804	−1363	−17.9	9.2
6	H-abstraction	reactant	0.754			
		product	0.758			BH&HLYP
		TS_6	0.759	−1505	5.7	15.7
7	H-abstraction	reactant	0.791			
		product	0.758			BH&HLYP
		TS_7	0.764	−857	23.8	26.8
8	C−C addition	reactant	0.76			
		product	0.788			B3LYP
		TS_8	0.786	−550	14.5	20.0
9	C−C addition	reactant	0.795			
		product	0.788			B3LYP
		TS_9	0.796	−226	−26.5	6.1

temperature and pressure reference, m is the change of the number of moles from reactants to the transition state, k_b is the Boltzmann constant, h is the Planck constant, and $\Delta G_0^{\ddagger}$ is the change of the Gibbs free energy from reactants to the transition state where R is the gas constant. For kinetics purpose, Arrhenius rate coefficients $A \exp(-E_a/RT)$ is often used. From the definition of activation energy E_a, by eq ii, and the expression of the macroscopic rate coefficient eq i, the Arrhenius activation energy is linked to the enthalpy of activation. Then, this results for an ideal gas to the following expressions for $E_a(T)$ and $A(T)$:

$$E_a = RT^2 \frac{d \ln k}{dT} \quad \text{(ii)}$$

$$E_a = \Delta H^{\ddagger} + (1 - m)RT \quad \text{(iii)}$$

$$A = \exp(1 - m)\left(\frac{k_B T}{h}\right) \exp\left(\frac{\Delta S^{\ddagger}}{R}\right)\left(\frac{R'Tc_0}{p_0}\right)^{-\Delta m} c_0^{\Delta m} \quad \text{(iv)}$$

A scaling factor of 0.9614[42] was applied to correct the overestimated harmonic vibrational frequencies with B3LYP whereas zero-point vibrational energies were scaled with 0.9806.[42]

For the reactions involving hydrogen atoms, tunneling corrections to the TST rate constants were computed using the Wigner tunneling correction factor:[43]

$$\kappa(T) = 1 - \frac{1}{24}\left(\frac{h\nu_s}{k_B T}\right)^2 \quad \text{(v)}$$

where ν_s is the transition state imaginary frequency.

All vibrational modes other than the lowest-vibrational one are treated harmonically, and for the lowest frequency modes the partition functions were calculated by the hindered rotor approximation of Truhlar and Chuang.[44]

Basis set superposition error was taken into account with the counterpoise correction of Boys and Bernardi.[45]

As the system is large and the reactions studied are in the range 400−750 K for pressures above 1 atm, we consider that pressure dependence could be neglected.

According to eq i, the transition state must be located on free energy surfaces and not on potential surfaces at 0 K. Indeed, the Gibbs free energy surface is a function not only of the position of the atoms and electronic structure but also of temperature and pressure. Therefore, the transition state structure also varies with temperature and pressure (influence of pressure is neglected for this study as said earlier). This kind of rate constant calculation based on this method is called the "theory of variational state" and was highlighted to treat correctly unimolecular reactions with "loose" transition state.[46] However, this approach remains a very demanding time-computing method and thus the following procedure was applied to the C−H bond dissociation of the hydromethylnaphthyl radical, reaction (−1), which presents the "loosest" transition state among the reactions selected in this study:

On one hand, all variables except the reaction coordinate were optimized whereas the reaction coordinate was varied stepwise. The optimized structure was then used as initial structure for the next step on the reaction path. At each step the free energy of the system was calculated (computer-time demanding). The transition state was then located on the free energy surfaces according to the coordinates of the reaction (method 1). On the other hand, the maximum of this linear transit on the potential energy served as a starting structure in a transition state optimization using the transit guided quasi-Newton method, TGQN. Then TS geometry was submitted to a vibrational frequency analysis (method 2).

3. Results and Discussion

Results (calculated with method 2) for reactions 1−9 are displayed in Table 1. Barrier heights and heats of reaction are

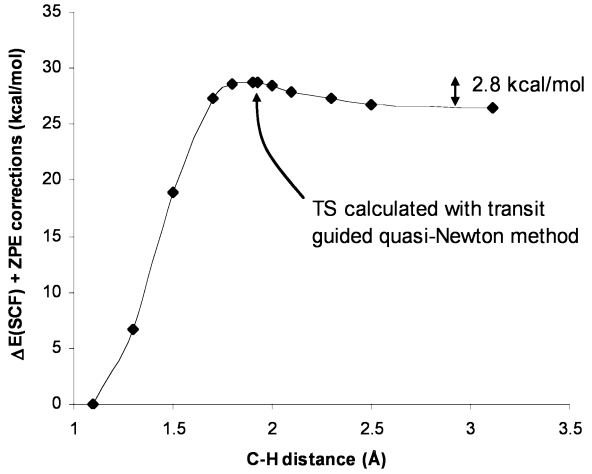

Figure 2. Potential energy surface of reaction −1 and location of its "quasi-loose" TS.

TABLE 2: Difference of $\Delta G^{\ddagger}$ (kcal/mol) and Rate Constants Ratio between Method 1 and 2 for Reaction −1

T (K)	400	450	500	550	600	650	700	750
$\Delta G_1^{\ddagger} - \Delta G_2^{\ddagger}$	−0.05	0.05	0.14	0.23	0.33	0.42	0.52	0.61
$k_1(T)/k_2(T)$	1.06	0.95	0.87	0.81	0.76	0.72	0.69	0.67

given including ZPE corrections. For all the reactions studied, the uDFT wave functions calculated did not suffer of large spin contamination, $\langle S^2 \rangle$ never exceeded 10% of the theoretical value. The location of the transition state with the TGQN method was confirmed by the only one imaginary frequency found by analysis of the vibrational frequencies. The imaginary frequencies are also displayed in Table 1 with a minus sign.

Method Justification. The reverse reaction (−1), dissociation of carbon-hydrogen bond, presents the most "loose" transition state among the reactions studied, as indicated in Table 1. This reaction was modeled following both methods. The "quasi-loose" transition state for (−1) is visible on the potential energy surface calculated on the reaction path according to the reaction coordinate in Figure 2. On this potential energy surface (PES) the maximum is also the TS_{-1} found by method 2. The distance of C−H dissociation of TS_{-1} found with method TGQN method on the potential energy surface is 1.925 Å.

After calculations of free energy at each point along the reaction path, the TS located on free energy surfaces no longer corresponded to the TS geometry found with method 2. The difference of free energy between the two methods in the range 400−750 K is given in Table 2. As expected, the free energy barrier found at low temperature by method 2 (TGQN) is a little higher than that calculated with method 1. This means that at low temperature, method 2 located better the TS structure than method 1 for which the TS structure was only "approximated" by successive bond stretches. However, as the TS geometry changes with increasing temperature, the free energy barrier calculated with method 2 becomes lower than the one calculated with method 1 above 420 K. Method 2 did not take into account the geometry changes of TS with temperature whereas method 1 approached better the TS location as the free energy was calculated for each bond stretch. However, this difference in free energy never exceeded 1 kcal/mol. The impact on the calculation of the rate constants is weak, $k_2(T)$ is only shifted by 1.06 at low temperature and 0.67 at 750 K, which is quite negligible, taking into account the uncertainty of calculations with B3LYP. Thus, the kinetic parameters calculated using the Arrhenius equation with both methods (Figure 3) are very close. The activation energy is higher with method 2 as the free energy

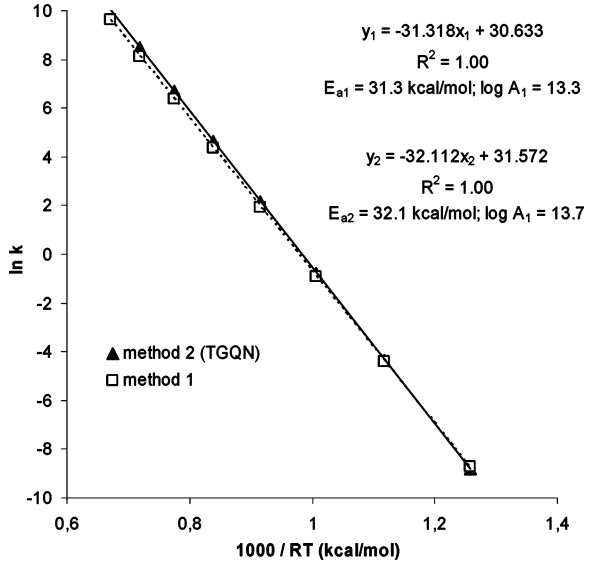

Figure 3. Arrhenius plots of ln $k(T)$ versus $1000/RT$ for reaction −1 with methods 1 and 2.

TABLE 3: Calculation of the Energy Barrier for Hydrogen Abstraction by H Atom on Benzene in kcal mol^{-1}

method	reactant	TS	barrier height
B3LYP (hartree)	−232.7586	−232.7407	11.27
BH&HLYP (hartree)	−230.2219	−230.1915	19.10
ZPE (kcal/mol)			−1.51
BSSE (kcal/mol)			0.35
barrier height (kcal/mol) at BH&HLYP with ZPE and BSSE corrections			17.92

barrier was higher at low temperature for method 2. But, due to the linear least-squares analysis of ln k versus $1/T$ (at 400−750 K) to calculate the Arrhenius parameters, it induced a higher preexponential factor for method 2 to compensate at high temperature the higher activation energy and then reflect thereafter the lower rate constants calculated with TGQN method compared to rate constant calculated with method 1 at higher temperature.

The location of the TS by the TGQN method has generated very little variation in the calculation of the rate constants compared to the location of the TS geometry on the free energy surfaces. Consequently, we have also modeled the other reactions in this study using method 2.

Additional calculations were performed for the reaction of hydrogen abstraction on benzene by the H atom. Geometries of reactants and TS were optimized with B3LYP. Thereafter, energies were calculated at the BH&HLYP level. ZPE and BSSE corrections were also estimated. The energy barriers calculated with both functionals are given in Table 3.

The final result for the barrier height is close to the corrected G2M value given by Mebel et al.[47] These authors estimated the energy barrier to be 17.5 kcal/mol. The heat of reaction, −7.5 kcal/mol can be compared to that calculated at a higher level of calculation, −8.7 ± 0.6 kcal/mol by these authors.[47] Our method gives also reliable bond distances for the TS geometry: C−H breaking bond and H−H forming bonds are respectively 1.478 and 0.857 Å. The three atoms involved in the reaction are almost linear, the angle C−H−H at TS is 179.8°. These values can again be compared to those of Mebel et al.[47] who found 1.48−1.49 and 0.846 Å for breaking and forming bonds.

3.1. Pathway A. Pathway A is induced by the release of hydrogen atoms in the system. Hydrogen atoms can either undergo an addition reaction or abstract another hydrogen atom on the reactant.

$$\mathrm{MNa} + \mathrm{H} \rightarrow \mathrm{HMNa} \quad (1)$$

$$\mathrm{MNa} + \mathrm{H} \rightarrow \mathrm{RMNa} + \mathrm{H_2} \quad (2)$$

Reaction 1, addition of a hydrogen atom on the naphthalenic ring, is exothermic by 26.6 kcal/mol and exhibits a low activation barrier of 4.4 kcal/mol. This value is in good agreement with the previous theoretical and experimental results on similar systems. Barckholtz et al.[27] determined a barrier energy of 3.77 kcal/mol for the hydrogen addition on benzene at the B3LYP/6-311+G(d,p) level. Park et al.[48] found an activation energy of 4.7 kcal/mol at the B3LYP/6-311G(d,p) level for the addition of hydrogen on biphenyl $C_{12}H_{10}$. Sauer et al.[49,50] gave activation energies of 3.3 and 4.3 kcal/mol by two separate experiments for the addition of hydrogen atom on benzene, and the energy barrier evaluated by Mebel et al.[47] (using G2M (rcc,MP2) level of theory) is higher, 8.9 kcal/mol. The experimental work by Nicovich[51] also give a low activation energy, 4.3 kcal/mol, and a similar rate constant for the addition of hydrogen atom on benzene in the range 400−750 K. The critical distance for the formation of C−H bond is 1.925 Å.

For reaction 2, two different types of hydrogen atoms can be considered for the hydrogen abstraction reaction: those from the aromatic moiety and those from the methyl group of 1-methylnaphthalene.

For the hydrogen abstraction of hydrogen of the methyl group, TS_2 geometry was found to be quasi linear, with a H−H−C angle of 5.1° and a H−H distance of 1.062 Å. The C−H distance of TS_2 is 1.247 Å. The energy barrier found was 7.4 kcal/mol (including ZPE corrections). The transition state exhibits an "early" character and the heat of reaction is about −16.4 kcal/mol. The reverse reaction is kinetically penalized as its energy barrier is about 23.8 kcal/mol, and thus, its influence in a kinetic scheme (for 400−750 K) is negligible for our system. The rate constants calculated for hydrogen abstraction are close, though slightly higher, to those determined on toluene[51−54] for hydrogen abstraction by hydrogen atom on toluene. This difference could be explained by the higher BDE (bond dissociation enthalpies) of the C−H bond of the methyl group of toluene compared to that for 1-methylnaphthalene[52] by 1.9 kcal/mol, resulting from a higher resonance stabilization for 1-methylnaphthalene. Taking into account this BDE difference in the calculation of the rate constants results in a very good agreement between the rate constants calculated for hydrogen abstraction for toluene and methylnaphthalene, as seen in Figure 4.

In Figure 5 are displayed rate constants of reactions 1 and 2 and also the rate constant of the hydrogen abstraction by H atoms on the aromatic ring. This type of reaction has recently received a lot of attention: such reactions are evoked as initiation reactions for the growth of polyaromatic compounds, notably benzene[27,47,41,55,56] and naphthalene:[41,56] in Figure 5, k_1 and k_2 are compared without adjustment to the rate constant calculated by Kislov et al.[56] who have also made B3LYP/6-31G(d,p) calculations. The rate constant of hydrogen abstraction of a hydrogen from the aromatic moiety calculated by these authors[56] was significantly lower than that from the methyl group and addition reaction at 400−750 K (Figure 5). Hydrogen abstraction from the aromatic moiety is thus minor compared to the one on the methyl group. The competition k_1/k_2 is

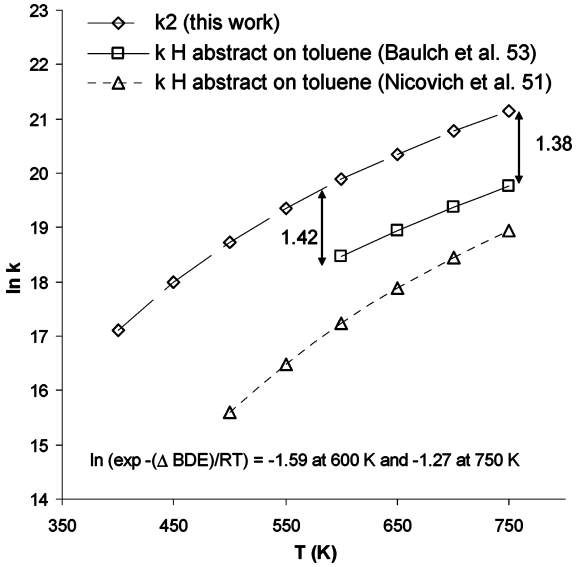

Figure 4. Comparison of rate constants ($dm^3\ mol^{-1}\ s^{-1}$) of reaction 2 and of hydrogen abstraction by H atom on toluene[51,53] between 400 and 750 K.

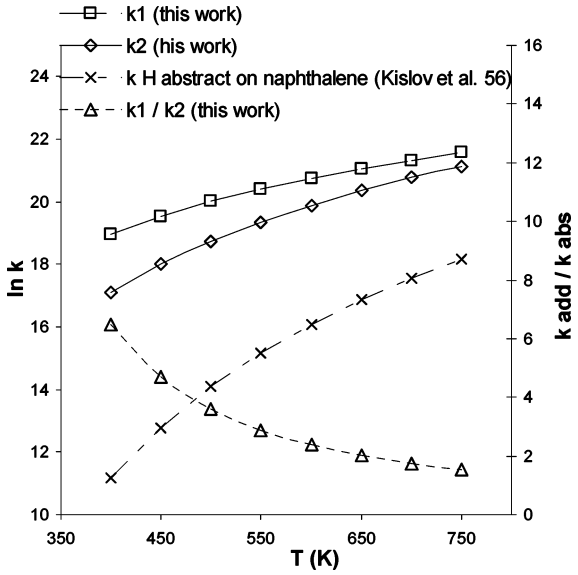

Figure 5. Rate constants ($dm^3\ mol^{-1}\ s^{-1}$) of reactions 1 and 2 between 400 and 750 K and the rate constant of hydrogen abstraction by H atom on naphthalene.[56]

favorable to the addition reaction in the range 400−750 K. The ratio k_1/k_2 decreases with increasing temperature as illustrated in Figure 5. This result is coherent with experimental data[51] and theoretical calculations[27] on toluene.

3.2. Pathway B.

$$\mathrm{HMNa} + \mathrm{MNa} \rightarrow \mathrm{MNa} + \mathrm{iHMNa} \quad (3)$$

$$\mathrm{HMNa} + \mathrm{MNa} \rightarrow \mathrm{H_3D1} \quad (4)$$

$$\mathrm{HMNa} \rightarrow \mathrm{H} + \mathrm{MNa} \quad (-1)$$

The RHT reaction (3) is a transfer of a β-hydrogen atom from a radical to an unsaturated closed-shell molecule. The energy barrier calculated was 26.5 kcal/mol. As reactant and product of this reaction present similarities, the heat of reaction is very low, only 1.6 kcal/mol. This reaction is exothermic on the whole temperature range studied, and thus this reaction favors hydrogenation in the ipso position (iHMNa). The geometry obtained

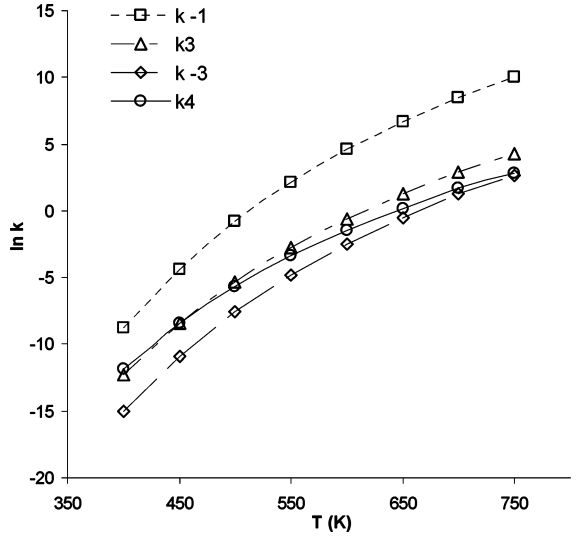

Figure 6. Rate constants of reactions 3, −3, 4 ($dm^3\ mol^{-1}\ s^{-1}$), and −1 (s^{-1}) between 400 and 750 K.

for TS_3 is almost linear: the C−H−C angle is 179.1° and the distance of the C−H bond being formed is 1.421 Å. A similar reaction was studied[57−59] for the system ethyl + ethylene. Franz et al.[57] have found at the uMP2/6-31G** level of theory an energy barrier of 27.2 kcal/mol, quite close to our value associated with a slightly shorter C−H bond length in the TS, 1.356 Å. Heuts et al.[58] have found at the G2(MP2) level of theory an energy barrier of 30.04 kcal/mol and a preexponential factor (at 298.15 K for both parameters) of $3.7 \times 10^8\ dm^3\ mol^{-1}\ s^{-1}$; the corresponding geometrical parameters of the TS geometry were a C−H−C angle of 171.9° and a C−H distance of 1.397 Å. Watts et al.[59] also studied this reaction with several methods (coupled-cluster, uMP2), and they estimated the RHT energy barrier at 298 K between 27.7 and 30.7 kcal mol^{-1}. Comparison with the system ethyl radical + ethylene is in good agreement with the previous studies:[57−59] the higher resonance stabilization of naphthalene lowers the energy barrier (by 1−3 kcal/mol) of the reaction for the methylnaphthalene system.

A competitive reaction to (3) is the addition of the HMNa radical to 1-methylnaphthalene, reaction 4. This reaction was evoked[60−64] to explain the formation of biaryl compounds during the pyrolysis of some PAH. The length of the forming bond of TS_4 is 2.111 Å, corresponding to a stretching of 32% compared to the dimer formed, H_3D1. The heat of reaction is 10.3 kcal/mol, and the energy barrier 23.1 kcal/mol. Thus reaction 4 can be competitive to reaction 3.

The third reaction of pathway B is the unimolecular dissociation of the carbon−hydrogen bond, the reverse reaction of (1), already described to justify the methodology employed. This dissociation exhibited an energy barrier of 29.3 kcal/mol.

If the energy barriers of reactions 3 and 4 are significantly lower than those of the dissociation reaction (from 2.8 to 6.2 kcal/mol lower), the rate constants have to be taken into consideration because the unimolecular dissociations are often characterized by high preexponential factors. The contribution of the entropic term in the expression of the rate constant is very low; the energy barrier on Gibbs energy only increases by 1.1 kcal/mol from 300 to 1200 K. The rate constants of reactions 3, −3, 4, and −1 versus temperature are displayed in Figure 6: as the ipso hydrogenated isomer iHMNa is more stable than HMNa at 400−750 K, k_3 is higher than k_{-3} on the whole temperature range. Due to their lower energy barriers, reactions 3 and 4 become more competitive to reaction −1 as the temperature decreases. Nevertheless, k_{-1} is higher than k_3 and k_4 at 400−750 K. If rate constant values indicate that reaction −1 is the faster reaction of this competitive node, one has to note that the concentration of reactant will also affect the rate of formation of iHMNa compared to the rate of reactions 3 and 4. Figure 7 displays for example the ratio between rates of reactions −1 and 3, r_{-1} and r_3, as a function of the initial reactant concentration, MNa_0,. Thus, except for very high concentration of reactant, the rate of reaction −1 is higher than the rate of reaction 3 at 400−750 K.

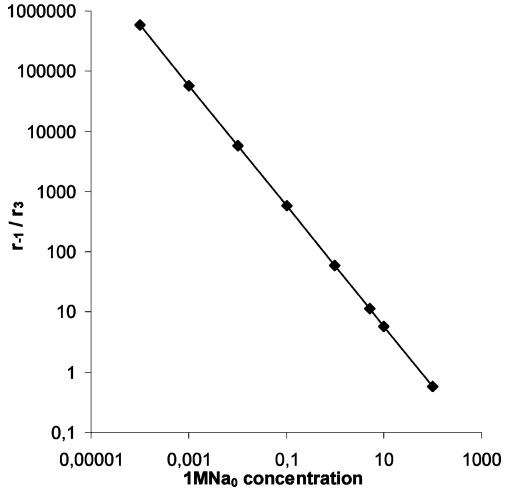

Figure 7. Ratio between the rates of reactions −1 and 3 in function of initial concentration of 1-MNa in mol L^{-1} at 450 K.

The ipso hydromethylnaphthyl radical (iHMNa) is formed consecutively to RHT (3) or the addition reaction (1). This latter radical releases a methyl radical through a carbon−carbon bond cleavage.[19] The methyl radicals can next abstract a hydrogen from methylnaphthalene producing methane and either RMNa radical (5) or naphthylmethyl radical MNRa (6).

$$MNa + {}^{\bullet}CH_3 \rightarrow RMNa + CH_4 \quad (5)$$

$$MNa + {}^{\bullet}CH_3 \rightarrow MNRa + CH_4 \quad (6)$$

Reaction 6 is thermodynamically less likely than (5), this latter being 17.9 kcal/mol exothermic instead of 5.7 kcal/mol endothermic for reaction 6. Hence, reverse reaction −5 can be discriminated for the same reason as reaction −2, its energy barrier is quite high, 27.1 kcal/mol. Lengths of forming and breaking bonds in both TS were consistent with those results: for the easier hydrogen abstraction, the bond being formed is longer than the bond being broken (respectively 1.469 and 1.263 Å) whereas the contrary was observed for TS_6 geometry, the bond being formed is shorter than the bond being broken (they were respectively 1.312 and 1.372 Å). In the same way, the H−C−H angle of the methyl group of TS_6 geometry was inferior to that of reaction 5 by 2°. As expected, hydrogen abstraction of "aromatic" hydrogen is less favorable than abstraction of methyl hydrogen: the respective energy barriers calculated were 9.2 and 15.7 kcal/mol. These values are close to those found experimentally on toluene, around 7−9.5 kcal/mol. At the best of our knowledge, no experimental or theoretical data are available for the hydrogen abstraction by methyl radicals on 1-methylnaphthalene. Consequently, k_5 is compared to the rate constants calculated for the hydrogen abstraction of methyl radical on toluene[65−67] (Figure 8). Our calculated rate constant is in good agreement with experimental data.[65−67]

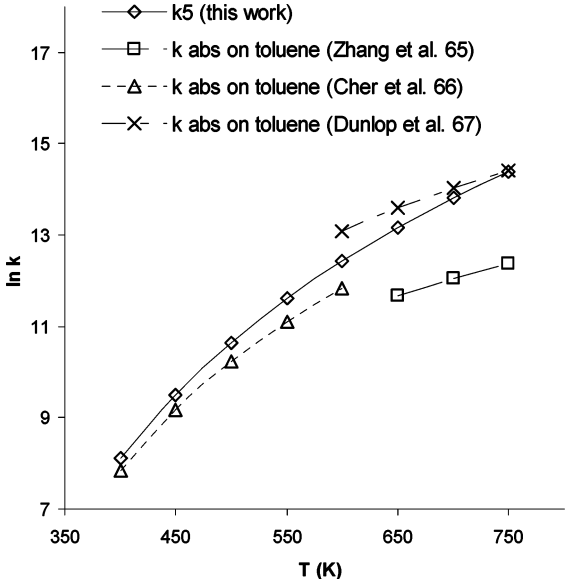

Figure 8. Comparison of rate constants ($dm^3\ mol^{-1}\ s^{-1}$) of reaction 5 calculated in this work and hydrogen abstraction by methyl radicals on toluene[65−67] between 400 and 750 K.

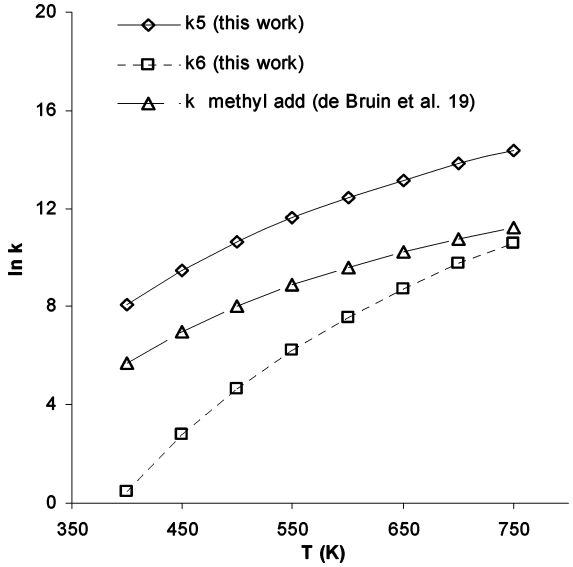

Figure 9. Rate constants of reactions 5 and 6 and of methyl addition on 9-methylphenanthrene[19] ($dm^3\ mol^{-1}\ s^{-1}$) between 400 and 750 K.

The abstraction of hydrogen by reaction 5 is thus highly favored compared to reaction 6. Variations of k_5 and k_6 as function of temperature are displayed in Figure 9, together with the rate constant of the reaction of methyl addition on 9-methylphenanthrene[19] calculated at uB3LYP/6-31G(d,p) level of theory. This latter rate constant is significantly lower than k_5, which is in good agreement with experimental results:[4,7] the production of methane was significantly higher than formation of dimethylaromatic compounds. Indeed, the ratio between rate constants of hydrogen abstraction by methyl radicals and addition of methyl radicals on the aromatic moiety is 10 at 400 K and 25 at 750 K. As for the competition addition/abstraction of H atom, methyl addition is more favorable at low temperature. On the contrary, hydrogen abstraction of an hydrogen of the aromatic ring becomes competitive with addition reaction of the methyl radicals above 600 K (Figure 9).

3.3. Pathway C.

$$\text{RMNa} + \text{MNa} \rightarrow \text{MNa} + \text{MNRa} \quad (7)$$

$$\text{RMNa} + \text{MNa} \rightarrow \text{HD3} \quad (8)$$

$$\text{MNRa} + \text{MNa} \rightarrow \text{HD1} \quad (9)$$

RMNa radicals produced by reactions 2 and 5 can afterward be involved in hydrogen abstraction (7), recombination, and addition reactions with 1-MNa (8) to form respectively MNRa radicals, 1,1′-dinaphthylethane (D2), and the hydromethyldinaphthylmethane radical, HD3. Through reaction 9, MNRa radicals undergo addition reaction with 1-methylnaphthalene and form hydrodimethylbinaphthyl radical, HD1. HD1 and HD3 radicals can form respectively D1 and D3 dimers by loss of hydrogen.

Reaction 7 is endothermic, the heat of reaction is of 23.8 kcal/mol in favor of the RMNa radical. This quite high activation energy is explained by the significant improved resonance stability of RMNa compared to MNRa. The energy barrier is of 26.8 kcal/mol. Thus, the reverse reaction (−7) exhibited a very low-energy barrier, 3.9 kcal/mol and is very fast.

Reaction 8 corresponds to the addition of RMNa to 1MNa. This reaction is 14.5 kcal/mol endothermic. The geometry of TS_8 exhibits rather a late, reactant-like character: the distance of C−C forming bond at the TS_8 geometry is 2.076 Å, and the HCH angle of the methyl radical group only decreases by 3°, from 116.8° for RMNa to 113° at TS_8 and against 106.2° for HD3. The barrier energy calculated was 20 kcal/mol.

MNRa radicals can after their formation undergo addition reaction on 1MNa (9). This reaction is 26.5 kcal/mol exothermic, and thus its TS_9 has an early, reactant-like character. The length of the forming bond of TS_9 is 2.284 Å whereas this bond length is 1.539 Å for the product. The dihedral angle formed by the attacked carbon and the aromatic ring is only 1.6° at TS_9. The dihedral angle between the hydrogen bonded to the attacked carbon and the aromatic ring presented the most important deviation, 12.9°. The energy barrier calculated is 6.1 kcal/mol, a value close to those already calculated for this kind of reactions on similar chemical system.[28−30,53,68,69] For example, Baulch et al.[53] determined from an extensive literature review an activation energy of 7.35 kcal/mol for the addition of methyl radical on ethylene, a value similar to the 8.8 kcal/mol activation energy we found for the addition of MNRa on MNa.

In Table 4 are displayed the values of rate constants involved in pathway C in the temperature range 400−750 K.

The recombination reaction between two methylnaphthyl radicals must also be considered. This type of reaction has received much attention, notably the methyl, ethyl, and benzyl recombination.[70−76] Most of these reactions have been reported with no energy barrier or very low-energy barrier. The rate constants calculated in function of the system are given in Table 5. Most of these values are very close to the experimental value obtained by Boyd et al.[73] for the recombination of two benzyl radicals.

Discriminate between those reactions to highlight the main mechanism responsible of the formation of dimers of 1-methylnaphthalene is not obvious. Indeed, it is difficult to conclude on the competition between the rates of formation of D1, D2, and D3 without considering a kinetic scheme: the radicals involved in the dimers formation are also involved in other elementary reactions, which are in competition. Thus relative concentrations, including the one of the reactant, may have an important role.

3.4. Calculation of Kinetic Parameters. Above calculations have then lead to the evaluations of rate constants of the reactions displayed in Figure 1 (except for the recombination between two methylnaphthyl radicals) at 400−750 K. Results are recapitulated in Table 6. From them and by means of eqs

TABLE 4: Calculated Rate Constants of Reactions 7, −7, 8, −8, 9, and −9 at 400−750 K in dm^3 mol^{-1} s^{-1} or s^{-1}

	400 K	450 K	500 K	550 K	600 K	650 K	700 K	750 K
k_7	2.73×10^{10}	1.70×10^{-8}	4.77×10^{-7}	7.53×10^{-6}	7.67×10^{-5}	5.58×10^{-4}	3.73×10^{-3}	1.4×10^{-2}
k_{-7}	9.75×10^{2}	2.35×10^{3}	4.93×10^{3}	9.33×10^{3}	1.63×10^{4}	2.67×10^{4}	4.49×10^{4}	6.18×10^{4}
k_8	8.58×10^{-6}	1.70×10^{-4}	1.91×10^{-3}	1.42×10^{-2}	7.71×10^{-2}	3.29×10^{-1}	1.26×10^{0}	3.51×10^{0}
k_{-8}	1.1×10^{7}	5.56×10^{7}	2.06×10^{8}	6.03×10^{8}	1.49×10^{9}	3.2×10^{9}	6.21×10^{9}	1.1×10^{10}
k_9	1.06×10^{3}	3.25×10^{3}	8.24×10^{3}	1.82×10^{4}	3.62×10^{4}	6.61×10^{4}	1.22×10^{5}	1.81×10^{5}
k_{-9}	1.66×10^{-3}	1.97×10^{-1}	9.18×10^{0}	2.17×10^{2}	3.06×10^{3}	2.90×10^{4}	2.01×10^{5}	1.09×10^{6}

TABLE 5: Reported Rate Constants of Recombination Reactions

reaction	$k(T)$	T (K)	ref
$CH_3 + CH_3$	$1.62 \times 10^{-10}(T/298\ \mathrm{K})^{-1.20} \exp(-590/RT)$ cm^3 molecule^{-1} s^{-1}	296−1800	71
$CH_3 + CH_3$	$1.69 \times 10^{-10}(T/298\ \mathrm{K})^{-1.10} \exp(-640/RT)$ cm^3 molecule^{-1} s^{-1}	1200−1600	72
$CH_3 + CH_3$	$1.91 \times 10^{-10}(T/298\mathrm{K})^{-1.17} \exp(-640/RT)$ cm^3 molecule^{-1} s^{-1}	200−2000	73
$C_7H_7 + C_7H_7$	$10^{7.4} \exp(1673/RT)$ L mol^{-1} s^{-1}	300−1200	19
$C_7H_7 + C_7H_7$	2.91×10^{-11} cm^3 molecule^{-1} s^{-1}	435−519	74
$C_7H_7 + C_7H_7$	$4.07 \times 10^{-12}(T/298\ \mathrm{K})^{0.4}$ cm^3 molecule^{-1} s^{-1}	300−1500	75
$C_7H_7 + C_7H_7$	2.09×10^{-13} cm^3 molecule^{-1} s^{-1}	300−843	76
$C_7H_7 + C_7H_7$	1.32×10^{-9} cm^3 molecule^{-1} s^{-1}	773−1020	77

TABLE 6: Calculated Rate Constants for Reactions 1−9 at the uB3LYP/6-31G and BH&HLYP/6-31G** Levels of Theory between 400 and 750 K**

reaction	k(400)	k(450)	k(500)	k(550)	k(600)	k(650)	k(700)	k(750)
1	1.74×10^{8}	3.07×10^{8}	4.91×10^{8}	7.32×10^{8}	1.03×10^{9}	1.40×10^{9}	1.83×10^{9}	2.32×10^{9}
−1	1.52×10^{-4}	1.29×10^{-2}	4.60×10^{-1}	8.66×10^{0}	1.01×10^{2}	8.16×10^{2}	4.91×10^{3}	2.34×10^{4}
2	2.68×10^{7}	6.54×10^{7}	1.36×10^{8}	2.54×10^{8}	4.33×10^{8}	6.91×10^{8}	1.04×10^{9}	1.51×10^{9}
3	4.81×10^{-6}	2.23×10^{-4}	4.95×10^{-3}	6.40×10^{-2}	5.52×10^{-1}	3.48×10^{0}	1.86×10^{1}	6.92×10^{1}
−4	3.01×10^{-7}	1.86×10^{-5}	5.15×10^{-4}	8.07×10^{-3}	8.15×10^{-2}	5.88×10^{-1}	3.52×10^{0}	1.45×10^{1}
4	2.07×10^{4}	5.53×10^{5}	7.46×10^{6}	6.60×10^{7}	4.01×10^{8}	1.85×10^{9}	7.47×10^{9}	2.16×10^{10}
−5	3.42×10^{5}	2.60×10^{6}	1.32×10^{7}	5.01×10^{7}	1.53×10^{8}	3.97×10^{8}	9.00×10^{8}	1.83×10^{9}
5	3.33×10^{3}	1.34×10^{4}	4.21×10^{4}	1.11×10^{5}	2.53×10^{5}	5.22×10^{5}	1.07×10^{6}	1.75×10^{6}
6	1.63×10^{0}	1.65×10^{1}	1.08×10^{2}	5.14×10^{2}	1.94×10^{3}	6.09×10^{3}	1.79×10^{4}	3.99×10^{4}
k_7	2.73×10^{10}	1.70×10^{-8}	4.77×10^{-7}	7.53×10^{-6}	7.67×10^{-5}	5.58×10^{-4}	3.73×10^{-3}	1.4×10^{-2}
k_{-7}	9.75×10^{2}	2.35×10^{3}	4.93×10^{3}	9.33×10^{3}	1.63×10^{4}	2.67×10^{4}	4.49×10^{4}	6.18×10^{4}
k_8	8.58×10^{-6}	1.70×10^{-4}	1.91×10^{-3}	1.42×10^{-2}	7.71×10^{-2}	3.29×10^{-1}	1.26×10^{0}	3.51×10^{0}
k_{-8}	1.1×10^{7}	5.56×10^{7}	2.06×10^{8}	6.03×10^{8}	1.49×10^{9}	3.2×10^{9}	6.21×10^{9}	1.1×10^{10}
k_9	1.06×10^{3}	3.25×10^{3}	8.24×10^{3}	1.82×10^{4}	3.62×10^{4}	6.61×10^{4}	1.22×10^{5}	1.81×10^{5}
k_{-9}	1.66×10^{-3}	1.97×10^{-1}	9.18×10^{0}	2.17×10^{2}	3.06×10^{3}	2.90×10^{4}	2.01×10^{5}	1.09×10^{6}

TABLE 7: Kinetic Parameters on the Scale 400−750 K

reaction	E_a, kcal/mol	log A, s^{-1} or L mol^{-1} s^{-1}	R^2
1	4.4	10.6	0.9988
−1	32.1	13.7	1
2	6.9	11.2	0.9991
3	28.1	10.0	0.9999
−3	30.2	9.9	0.9999
4	25.1	8.5	1
−4	14.6	13.5	1
5	10.7	9.3	0.9989
6	17.3	9.6	0.9996
7	30.3	6.9	0.9999
−7	7.1	6.8	0.9972
8	22.1	6.9	0.9998
−8	11.8	13.5	1
9	8.8	7.8	0.9997
−9	34.6	16.1	0.9983

iv and v, the Arrhenius parameters were calculated by fitting a linear function through the values of $k(T)$ with a least-squares method. Activation energies, E_a, and preexponential factors are displayed in Table 7. In the low range of temperature chosen, E_a and A can be considered constant with temperature, the correlation coefficients (R^2) calculated were found very close to 1 for each reaction. These kinetic parameters can then be integrated into a kinetic scheme accounting for 1_MNa thermal degradation

4. Conclusion

We have applied density functional B3LYP and BH&HLYP methods with the 6-31G** basis set combined with transition state theory to calculate rate constants of reactions involved during 1-methylnaphthalene pyrolysis. ZPE and BSSE were taken into account to estimate barrier heights. Reaction pathways were investigated with competitive reactions by implying three radicals, hydrogen atom, hydromethylnaphthyl, and methylnaphthyl radicals and the reactant. Rate constants were calculated in the range 400−750 K, from the geological conditions to those of the laboratory. The method and level of theory chosen gave reliable results in agreement with previous theoretical studies or experimental data.

For pathway A, the addition reaction of H atm on 1-MNa is favored over abstraction hydrogen at low temperature. This result is in good agreement with previous experimental work,[7] for which a significant yield of molecular hydrogen was observed only at high severity of pyrolysis, i.e., at the latest stage of 1-methylnaphthalene pyrolysis. With increasing temperature, hydrogen abstraction becomes competitive to addition.

For pathway B, rate constants of reactions 3 and 4, RHT and formation of H_3D1, are lower than the rate constant of reaction −1. This behavior decreases with temperature, as $E_{a,3}$ and $E_{a,4}$ are lower than $E_{a,-1}$. The hydrogen abstraction of the methyl radical is done preferentially on hydrogens of the methyl group rather than on hydrogen of the aromatic moiety. Furthermore, the ratio between rate constants of hydrogen abstraction of hydrogen of the methyl group and addition of the methyl radicals[19] was about of 10 in the temperature range studied: dimethylnaphthalenes would be a minor product compared to methane.

For pathway C, reaction 9 exhibited the lowest activation energy. However, the discrimination between the predominant

rates of formation of dimers, D1, D2, and D3 needs to also consider reaction 4, which produces H_3D1 and reverse reactions −4, −8, and −9. As many reactions involve the radical precursors (HMNa, RMNa and MNRa) of dimers, the use of a kinetic scheme is necessary to take into account all the reactions, the initial concentration of reactant and the relative concentrations between radicals.

The next step to this study will be to test the complete kinetic scheme for the thermal conversion of 1-methylnaphthalene with the use of the kinetic parameters calculated in this work. Discrimination between the predominant rates of formation for dimers will then be elucidated.

Acknowledgment. T. De Bruin and C. Dartiguelongue of French Institute of Petroleum are acknowledged for fruitful discussions and advice. We benefited greatly from the careful reviews and helpful comments of the two anonymous reviewers.

References and Notes

(1) Tissot, B. P.; Welte, D. H. *Petroleum Formation and Occurrence*, 2nd ed.; Springer-Verlag: Berlin, 1984.
(2) Lorant, F.; Behar, F.; Vandenbroucke, M.; McKinney, D. E.; Tang, Y. *Energy Fuels* **2000**, *14*, 1143−1155.
(3) Gräber, W-D.; Hüttinger, K. J. *Fuel* **1982**, *61*, 505−509.
(4) Behar, F.; Budzinski, H.; Vandenbroucke, M.; Tang, Y. *Energy Fuels* **1999**, *13* (2), 471−481.
(5) Smith, C. M.; Savage, P. E. *AIChE J.* **1993**, *39*, 1355−1360.
(6) Smith, C. M.; Savage, P. E. *Energy Fuels* **1992**, *6*, 195−202.
(7) Leininger, J. P.; Minot, C.; Lorant, F.; Behar, F. *Energy Fuels* **2006**, *20* (6), 2518−2530.
(8) Glasstone, S.; Laidler, K. J.; Eyring, H. *The Theory of Rate Processes*; McGraw-Hill: New York, 1941.
(9) McIver, J. W.; Kormonicki, A. *J. Am. Chem. Soc.* **1972**, *94*, 2625−2634.
(10) Bobrowicz, F. W.; Goddard, W. A., III. *Modern Theoretical Chemistry: Methods of Electronic Structure Theory*; Schaefer, H. F., III, Ed.; Plenum: New York, 1977; Chapter 4.
(11) Abashkin, Y.; Russo, N. J. *Chem. Phys.* **1994**, *100* (6), 4477.
(12) Peng, C.; Schlegel, H. B. *Isr. J. Chem.* **1994**, *33*, 449−454.
(13) McMillen, D. F.; Malhotra, R.; Hum, G. P.; Chang, S.-J. *Energy Fuels* **1987**, *1*, 193−198.
(14) Malhotra, R.; McMillen, D. F. *Energy Fuels* **1990**, *4*, 184−193.
(15) Poutsma, M. L. *Energy Fuels* **1990**, *4*, *2*, 113−131.
(16) Malhotra, R.; McMillen, D. F. *Energy Fuels* **1993**, *7*, 227−233.
(17) Savage, P. E. *Energy Fuels* **1995**, *9*, 590−598.
(18) Poutsma, M. L. *J. Anal. Appl. Pyrol.* **2000**, *54*, 5−35.
(19) de Bruin, T. J. M.; Lorant, F.; Toulhoat, H.; Goddard, W. A., III. *J. Phys. Chem. A.* **2004**, *108* (46), 10302−10310.
(20) Jaguar 5.5 and 6.5; Schrödinger, Inc.: Portland, OR, 1991−2005.
(21) Parr, R. G.; Yang, W. *Density-Functional Theory of Atoms and Molecules*; Oxford University Press: New York, 1989.
(22) Becke, A. D. *J. Chem. Phys.* **1992**, *96*, 2155. Becke, A. D. *J. Chem. Phys*. **1992**, *97*, 9173. Becke, A. D. *J. Chem. Phys.* **1993**, *98*, 5648.
(23) Lee, C.; Yang, W.; Parr, R. G. *Phys. Rev.* **1988**, *B37*, 785.
(24) Hehre, W. J.; Ditchfield, R.; Pople, J. A. *Chem. Phys.* **1972**, *56*, 2257.
(25) Smith, D. M.; Nicolaides, A.; Golding, B. T.; Radom, L. *J. Am. Chem. Soc.* **1998**, *120*, 10223−10233.
(26) Barckholtz, C.; Barckholtz, T. A.; Hadad, C. M. *J. Phys. Chem. A* **2001**, *105*, 140−152.
(27) Barckholtz, C.; Barckholtz, T. A.; Hadad, C. M. *J. Am. Chem. Soc.* **1999**, *121* (3), 491−500.
(28) Richter, H.; Mazyar, O. A.; Sumathi, R.; Green, W. H.; Howard, J. B.; Bozzelli, J. W. *J. Phys. Chem. A* **2001**, *105*, 1561−1573.
(29) Verrecken, L.; Peeters, J.; Bettinger, H. F.; Kaiser, R. I.; von Schleyer, P. R; Schaefer, H. F., III. *J. Am. Chem. Soc*. **2002**, *124*, 2781.
(30) Verrecken, L.; Peeters, J. *Phys. Chem. Chem. Phys.* **2003**, *5*, 2807−2817.
(31) Kandanarachchi, P. H.; Autrey, T.; Franz, J. A. *J. Org. Chem.* **2002**, *67*, 7937−7945.
(32) Zheng, X. L.; Sun, H. Y.; Law, C. K. *J. Phys. Chem. A* **2005**, *109*, 9044−9053.
(33) Sun, H.; Bozzelli, J. W. *J. Phys. Chem. A* **2004**, *108*, 1694−1711.
(34) Miehlich, B.; Savin, A.; Stoll, H.; Preuss, H. *Chem. Phys. Lett.* **1989**, *157*, 200−206.
(35) Adamo, C.; Barone, V. *J. Chem. Phys.* **1998**, *108*, 664−675.
(36) Boese, A. D.; Martin, J. M. L. *J. Chem. Phys.* **2004**, *121*, 3405−3416.
(37) Zhang, Q.; Bell, R.; Truong., T. N. *J. Phys. Chem.* **1995**, *99*, 592.
(38) Durant., J. L. *Chem. Phys. Lett.* **1996**, *256*, 595.
(39) Lynch, B. J.; Fast, P. L.; Harris, M.; Truhlar, D. G. *J. Phys. Chem. A* **2000**, *104*, 4811−4815.
(40) Lynch, B. J.; Truhlar, D. G. *J. Phys. Chem. A* **2001**, *105*, 2936−2941.
(41) Violi., A.; Truong, T. N.; Sarofim, A. F. *J. Phys. Chem. A* **2004**, *108*, 4846−4852.
(42) Scott, A. P.; Radom, L. *J. Phys. Chem.* **1996**, *100*, 16502−16513.
(43) Wigner, E. P. Z. *Phys. Chem.* **1932**, *B19*, 203.
(44) Truhlar, D. G. *J. Comp. Chem.* **1991**, *12*, 266−270.
(45) Boys, S. F.; Bernardi, F. *Mol. Phys.* **1970**, *19*, 553.
(46) Hase, W. L. *Acc. Chem. Res.* **1983**, *16*, 258.
(47) Mebel, A. M.; Lin, M. C.; Yu, T.; Morokuma, K. *J. Phys. Chem. A* **1997**, *101*, 3189.
(48) Park, J.; Nam, G. J.; Tokmakov, I. V.; Lin, M. C. *J. Phys. Chem. A* **2006**, *110* (28), 8729−8735.
(49) Sauer, M. C., Jr.; Ward, B. *J. Phys. Chem.* **1967**, *71*, 3971−3983.
(50) Sauer, M. C., Jr.; Mani, I. *J. Phys. Chem.* **1970**, *74*, 59−63.
(51) Nicovich, J. M.; Ravishankara, A. R. *J. Phys. Chem.* **1984**, *88*, 2534−2541.
(52) Ellis, C.; Scott, M. S.; Walker, R. W. *Combust. Flame* **2003**, *132*, 291.
(53) Baulch, D. L.; Cobos, C. J.; Cox, R. A.; Frank, P.; Hayman, G.; Just, Th.; Kerr, J. A.; Murrells, T.; Pilling, M. J.; Troe, J.; Walker, R. W.; Warnatz, J. *J. Phys. Chem. Ref. Data* **1994**, *23*, 847.
(54) Stein, S. E.; Brown, R. L. *J. Am. Chem. Soc.* **1991**, *113*, 787.
(55) Bauschlicher, C. W.; Ricca, A. *Chem. Phys. Lett.* **2000**, *326*, 283.
(56) Kislov, V. V.; Mebel, A. M.; Lin, S. H. *J. Phys. Chem. A* **2002**, *106*, 6171−6182.
(57) Franz, J. A.; Ferris, K. F.; Camaioni, D. M.; Autrey, S. T. *Energy Fuels* **1994**, *8*, 1016−1019.
(58) Heuts, J. P. A.; Pross, A.; Radom, L. *J. Phys. Chem.* **1996**, *100*, 17087−17089.
(59) Watts, J. D.; Franz, J. A.; Bartlett, R. J. *Chem. Phys. Lett.* **1996**, *249*, 496−500.
(60) Stein, S. E. *Carbon* **1981**, *19*, 6, 421−429.
(61) Stein, S. E.; Griffith, L. L.; Billmers, R.; Chen, R. H. *J. Org. Chem.* **1987**, *52*, 1582−1591.
(62) Stein, S. E.; Brown, R. L.; Griffith, L. L.; Manka, M. *J. Am. Chem. Soc.* **1984**, *29*, 2, 42−48.
(63) Dasgupta, R.; Maiti, B. R. *Ind. Eng. Chem. Process Des. Dev.* **1986**, *25*, 381−386.
(64) Leyssale, F. Etude de la pyrolyse d'alkylpolyaromatiques appliquées aux procédés de conversion des produits lourds du pétrole. Université Paris VI, 1991.
(65) Zhang, H. X.; Ahonkhai, S. I.; Back, M. H. *Can. J. Chem.* **1989**, *67*, 1541−1549.
(66) Cher, M.; Hollingsworth, C. S.; Sicilio, F. *J. Phys. Chem.* **1966**, *70*, *3*, 877.
(67) Dunlop, A. N.; Kominar, R. J.; Price, S. J. W. *Can. J. Chem.* **1970**, *48*, 1269.
(68) Van Speybroeck, V.; Van Neck, D.; Waroquier, M.; Wauters, S.; Sayes, M.; Marin, G. B. *J. Phys. Chem. A* **2000**, *104*, 10939.
(69) Tokmakov, I. V.; Lin, M. C. J. *Am. Chem. Soc.* **2003**, *125*, 11397−11408.
(70) Du, H.; Hessler, J. P.; Ogren, P. J. *J. Phys. Chem.* **1996**, *100*, 974−983.
(71) Hwang, S. M.; Wagner, H. G.; Wolff, Th. *Symp. Int. Combust. Proc.* **1991**, *23*, 99.
(72) Walter, D.; Grotheer, H. *Symp. Int. Combust. Proc.* **1991**, *23*, 107.
(73) Boyd, A. A.; Noziere, B.; Lesclaux, R. *J. Phys. Chem.* **1995**, *99*, 10815−10823.
(74) Muller-Markgraf, W.; Troe, J. *J. Phys. Chem.* **1988**, *92*, 4899.
(75) Benson, S. W.; Weissman, M. *Int. J. Chem. Kinet.* **1982**, *14*, 1287.
(76) Ebert, K. H.; Ederer, H. J.; Schmidt, P. S. *Chemical Reaction Engineering-Houston*; Weekman, V. W., Jr., Luss, D., Eds.; ACS Symposium Series 65; American Chemcial Society: Washington, DC, 1978; pp 313−324.